ELSEVIER

Journal of Nuclear Materials 297 (2001) 345–354

journal of nuclear materials

www.elsevier.com/locate/jnucmat

Temperature effects on the radiation stability and ion exchange capacity of smectites

B.X. Gu [a], L.M. Wang [a], L.D. Minc [b], R.C. Ewing [a,*]

[a] *Department of Nuclear Engineering and Radiological Sciences, Cooley Building, 2355 Bonisteel Boulevard, University of Michigan, Ann Arbor, MI 48109-2104, USA*

[b] *Phoenix Memorial Laboratory, University of Michigan, Ann Arbor, MI 48109-2104, USA*

Received 15 August 2000; accepted 9 May 2001

Abstract

Radiation stability of montmorillonite, nontronite, and saponite as a function of temperature has been investigated by in situ transmission electron microscopy (TEM) with 200 keV electrons. All three phases underwent a crystalline-to-amorphous transformation when exposed to electron beam irradiation over the temperature range of 25–750°C. At room temperature, the amorphization doses of montmorillonite, nontronite and saponite are 1.3×10^{24}, 6.2×10^{24} and 1.7×10^{24} e^-/m^2, which correspond to energy depositions of 3.0×10^{10}, 3.4×10^{11} and 6.0×10^{10} Gy, respectively. In the low-temperature region (25–400°C), the amorphization doses of all three types of smectite increase with the increase of temperature. Further increase of temperature to above 400°C leads to a decrease in the amorphization dose. The temperature effect on the ion exchange capacity for Cs has been studied using thermally treated smectites at temperatures between 25°C and 900°C. No change in ion exchange capacity was found at temperatures below 400°C, for which dehydration is the dominant process during the heat treatment. Above this temperature, dehydroxylation, amorphization and phase transformation occur depending on temperature. The ion exchange capacity decreases with the increase in temperature, as a result of the loss of exchangeable cations in the crystalline structure.

1. Introduction

Bentonite, consisting primarily of montmorillonite, is a common choice for barrier materials in high-level nuclear waste disposal [1,2]. In addition to creating favorable geochemical conditions around the waste canisters, bentonite can also serve as a hydraulic barrier to retard ground water contact and limit the mobility of radionuclides released from the waste forms after they come in contact with ground water. The low hydraulic conductivity, high swelling properties and high ion exchange and sorption capacity for the radionuclides, such as Cs^+, Sr^{2+}, rare-earths, and actinides, have made the smectite group of clay minerals among the most promising candidate backfill materials for geologic disposal [3–7]. Smectites have also been found as the important constituents of the alteration products on the corroded glass waste forms [8]. These surface layers may play a role in the retardation of radionuclides released from the glass waste form. Rare-earths, actinides, Cs, and Sr are retained in the smectites that form in this alteration layer through ion exchange reactions or sorption onto the smectite surface [8,9].

The conditions in the near field of a high-level waste disposal repository are severe in terms of radiation and temperature. Significant amounts of heat may be generated in the repository due to the β-decay of the fission products. The temperature rise in the near field of a repository may be significant based on the calculations made by Buscheck et al. [10]. For US defense high-level nuclear waste (HLW) glasses, an initial temperature as high as 250°C may be achieved in the Yucca Mountain repository. The temperature may

* Corresponding author. Tel.: +1-734 647 8529; fax: +1-734 647 8531.

E-mail address: rodewing@umich.edu (R.C. Ewing).

0022-3115/01/$ - see front matter
PII: S0022-3115(01)00631-6

drop slowly to below 100°C after several hundred years of storage. The temperature of the glass waste form itself can be even higher. The estimated waste form temperature is in the range between 100°C and 450°C, depending on waste loading, age of the waste, depth of burial, and the repository-specific geothermal gradient [11].

Because smectites are hydrated sheet silicates, with most of the exchangeable cations and water molecules located in the interlayer positions, many important physical and chemical properties, such as the hydraulic conductivity, swelling and ion exchange capacities, are predominantly determined by the interlayer structure. The removal of water from the interlayer can lead to the collapse of the interlayer structure, migration of interlayer cations and new charge balance schemes in the layered structure. Reversible or irreversible dehydration accompanied by a significant decrease in interlayer spacing can occur when smectite is subjected to heating at temperatures below 400°C. Dehydroxylation and phase transformation occur in most of smectites when samples are heated at temperatures above 400–500°C [12–15].

The regulatory period for geologic repositories usually extends to at least 10 000 years. Thus, the near-field materials, such as smectites, may be exposed to a high radiation field for a long period of time. The radiation stability of the waste form and backfill materials is of critical importance in the assessment of their long-term behavior, because the radiation-induced structural damage may lead to changes in the physical and chemical properties, such as the thermal conductivity, ion exchange and sorption capacities. Both radiation and thermally induced amorphization can cause significant loss of ion exchange capacity for radionuclides such as Cs and Sr [16,17]. Radiation-induced amorphization and bubble formation have been observed in mica group minerals (with 2:1 sheet structure similar to that of smectites) under Kr^+ irradiation [18]. All of the mica minerals studied were amorphized at relatively low critical amorphization doses (a fraction of a dpa) at room temperature. Having a similar chemical composition and crystal structure to mica, smectites are likely to be susceptible to radiation damage.

The temperature field in a waste repository may also affect the radiation stability of the near-field materials. The temperature dependence of amorphization dose has been investigated for a variety of silicates. The amorphization dose of mica group minerals was found to increase with the increase of temperature [18], while zeolites showed a decreased amorphization dose when the irradiation temperature was increased [19]. The variation in radiation stability with temperature is associated with the particular structure and composition of the materials studied.

A systematic study, using thermal treatment and in situ transmission electron microscopy (TEM), has been performed to investigate the changes of smectite structure, ion exchange capacity and radiation stability with temperature. The smectites selected for the study are either the candidate backfill materials for a nuclear waste repository or phases that are found as corrosion products on the surface of glass waste forms. These phases also represent the materials from the two compositional subgroups (i.e. dioctahedral and trioctahedral sheet structures) of the smectite minerals.

2. Experimental

2.1. Materials

Smectite is a 2:1 clay mineral that consists of two tetrahedral layers with one octahedral layer between the tetrahedral layers. Charge deficiency in the 2:1 unit results from cation substitution in the tetrahedral or octahedral layers. The structural charges are balanced by introducing exchangeable cations into the interlayer position. Water molecules are readily adsorbed to form hydration shells around the interlayer cations. The structures of dioctahedral and trioctahedral smectites are depicted in Fig. 1. The three smectite phases studied include: (1) dioctahedral montmorillonite, (2) dioctahedral nontronite, and (3) trioctahedral saponite. The ideal formulas for the three types of smectite are [20]

montmorillonite $[K_{0.7}(Al_{3.3}Mg_{0.7})Si_8O_{20}(OH)_4 \cdot nH_2O]$,

nontronite $[K_{0.7}Fe_4(Si_{7.3}Al_{0.7})O_{20}(OH)_4 \cdot nH_2O]$,

saponite $[K_{0.8}Mg_6(Si_{7.2}Al_{0.8})O_{20}(OH)_4 \cdot nH_2O]$.

The montmorillonite from Apache County, AZ, USA and the nontronite from Cheney, WA, USA were provided by Ward's Natural Science Establishment in aggregated form. Both samples were ground and dry sieved through 60 mesh before ion exchange and thermal treatment. Saponite clay (SM 1200) was provided by GSA Resources in powdered form.

2.2. Thermal treatment and XRD analysis

All three types of material were thermally treated at temperatures in the range of 100–900°C for 1 h and then cooled to room temperature in air. The heat-treated samples were kept in a desiccator prior to use. The structures of the original and thermally treated smectites were examined with X-ray diffraction (XRD) using a Scintag X1 Automated Powder Diffractometer.

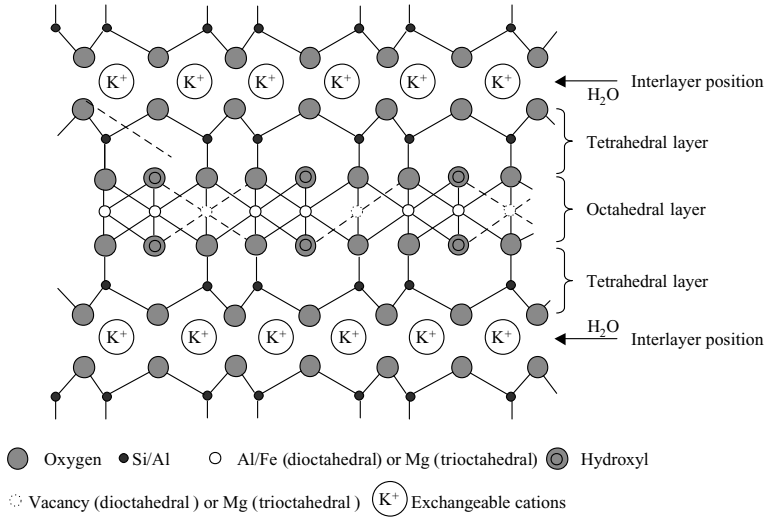

Fig. 1. Schematic diagram of the structure of dioctahedral and trioctahedral smectites.

2.3. Electron beam irradiation

Radiation damage in smectites under electron beam irradiation were observed in situ by TEM using a JEM 2000 FX electron microscope operated at 200 keV. A JEM 4000 EX electron microscope was also used to obtain high-resolution TEM images during the course of 400 keV electron beam irradiation of montmorillonite. The smectite samples were crushed and suspended on a $\varnothing$ 3 mm holey carbon film supported by a copper grid. The electron flux exposed on the smectite samples was determined based on the current density on the image screen with the electron beam aligned through a hole in the sample. The TEM samples were heated in a temperature range of 25–750°C, using a heating stage attached to the microscope during the electron irradiation.

2.4. Ion exchange

100 mg of the original and thermally treated smectites were dispersed in 25 ml 2 mN CsCl solution prepared by dissolving reagent grade CsCl in deionized water. The suspensions were continuously stirred on a shaker with an orbital speed of 150 rpm for 48 h with temperature maintained at room temperature. Centrifugation at 3500 rpm was used to separate the liquid phase from the solid when the ion exchange reaction was terminated. Samples of supernatant were analyzed for Cs^+ content using instrumental neutron activation analysis at the University of Michigan's Ford Nuclear Reactor. Approximately 200 mg of each solution were weighed out into a high-purity quartz vial and desiccated on filter paper. The encapsulated samples, along with 4 replicates of a standard reference material (Specpure Cesium plasma standard, 1000 ± 5 ppm solution), were irradiated for 20 h in a core-face location with an average thermal flux of 4.2×10^{16} n/m^2 s. After a 3 week decay, gamma activity from Cs-134g decay was recorded over a 10 000 s live-time count on an HPGe coaxial detector (34% relative efficiency). Cesium concentrations were then determined through direct comparison with three replicates of the standard reference material, using a fourth replicate as a check standard. The check indicated a total measurement error for cesium content at 2.9%.

3. Results and discussion

3.1. Radiation stability

The crystalline-to-amorphous transition of the smectites was observed using selected area electron diffraction (SAD) under TEM. Fig. 2 shows two sequences of SAD patterns obtained at different cumulative doses for nontronite and saponite irradiated with 200 keV electrons at room temperature. A similar sequence of diffraction patterns were also obtained for montmorillonite irradiated with 200 keV electrons as shown in Figs. 3(a)–(c). The sharp ring patterns obtained from the unirradiated smectites confirmed that the smectites were crystalline. The gradual loss of the ring pattern intensity accompanied by the appearance of the diffraction haloes, the characteristic of amorphous materials, with the increase of radiation dose indicates that the crystalline structure is progressively damaged. The disappearance of the sharp ring pattern at a certain dose is an indication that the crystalline structure has become completely

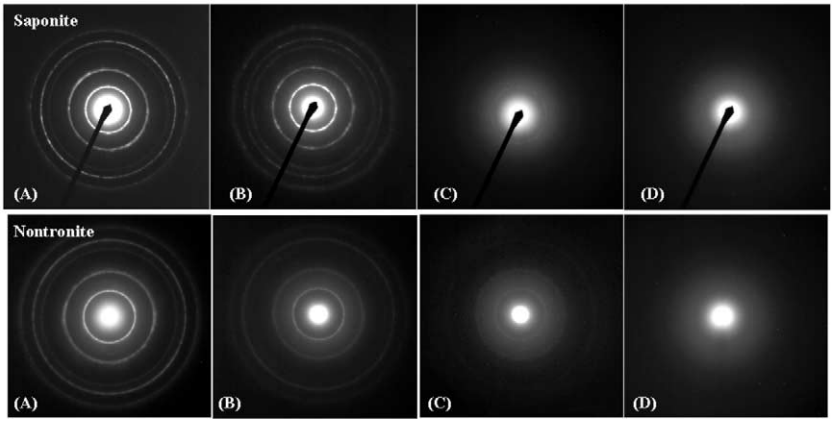

Fig. 2. SAD patterns of nontronite and saponite irradiated by a 200 keV electron beam. Saponite: (A) beginning of the irradiation; (B) 0.5×10^{24} e^-/m^2; (C) 1.3×10^{24} e^-/m^2; (D) 1.6×10^{24} e^-/m^2. Nontronite: (A) beginning of the irradiation; (B) 3×10^{24} e^-/m^2; (C) 4×10^{24} e^-/m^2; (D) 6×10^{24} e^-m^2.

disordered. The dose at which sharp rings have completely disappeared is defined as the critical amorphization dose. Figs. 3(d)–(f) are a sequence of high-resolution TEM images of montmorillonite, showing the evolution from layered structure to amorphous state. The crystalline-to-amorphous transition of smectite is further confirmed by the loss of the layered structure (e.g. absence of lattice fringes) with the increase of radiation dose in the high-resolution TEM images.

The temperature dependence of amorphization doses for the smectite phases were measured over a temperature range of 25–750°C. The crystalline-to-amorphous transition was observed in situ by TEM, with the amorphization dose recorded using the electrical current measured on the image screen and exposure time. All the amorphization doses were measured at the same dose rate of 1×10^{22} e^-/m^2 s in order to eliminate the dose rate effect. Table 1 summarizes the amorphization doses for the three types of smectites irradiated by a 200 keV electron beam at different temperatures. Because many important phenomena, including changes in physical properties or induced chemical reactions, are expected to scale as the energy absorbed per unit mass of the material rather than as the exposure dose, the critical electron fluences were converted to the ionizing energy deposition. The details of the calculation of energy deposition by incident electrons can be found elsewhere [19]. At room temperature, the amorphization doses of

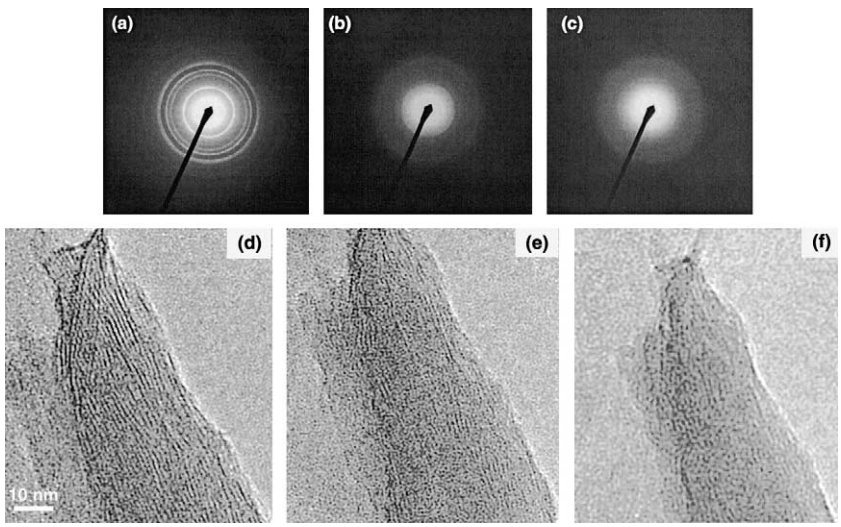

Fig. 3. SAD patterns (a)–(c) and high-resolution TEM images (d)–(f) of montmorillonite. Radiation doses corresponding to the diffraction patterns are: (a) beginning of the irradiation; (b) 0.8×10^{24} e^-/m^2; (c) 1.3×10^{24} e^-/m^2 (under 200 keV electron irradiation).

Table 1
Amorphization doses of smectites under 200 keV electron beam irradiation

Montmorillonite			Nontronite			Saponite		
Temperature (°C)	Electron fluence (e^-/m^2)	Energy deposition (Gy)	Temperature (°C)	Electron fluence (e^-/m^2)	Energy deposition (Gy)	Temperature (°C)	Electron fluence (e^-/m^2)	Energy deposition (Gy)
24	1.34×10^{24}	3.00×10^{10}	25	6.19×10^{24}	3.42×10^{11}	25	1.66×10^{24}	6.00×10^{10}
102	2.42×10^{24}	5.41×10^{10}	121	1.41×10^{25}	7.78×10^{11}	124	3.12×10^{24}	1.13×10^{11}
203	4.44×10^{24}	9.93×10^{10}	202	2.84×10^{25}	1.57×10^{12}	202	3.08×10^{24}	1.11×10^{11}
304	2.23×10^{25}	4.98×10^{11}	305	4.07×10^{25}	2.25×10^{12}	302	3.80×10^{24}	1.37×10^{11}
353	3.04×10^{25}	6.80×10^{11}	400	3.32×10^{25}	1.83×10^{12}	407	4.97×10^{24}	1.80×10^{11}
450	1.99×10^{25}	4.45×10^{11}	500	2.12×10^{24}	1.17×10^{11}	505	1.26×10^{24}	4.55×10^{10}
500	7.13×10^{24}	1.59×10^{11}	554	5.55×10^{24}	3.06×10^{11}	552	1.22×10^{24}	4.41×10^{10}
601	6.77×10^{24}	1.51×10^{11}	604	2.91×10^{24}	1.61×10^{11}	601	5.17×10^{23}	1.87×10^{10}

montmorillonite, nontronite and saponite are 1.3×10^{24}, 6.2×10^{24} and 1.7×10^{24} e^-/m^2, which correspond to energy depositions of 3.0×10^{10}, 3.4×10^{11} and 6.0×10^{10} Gy, respectively. These values are on the same order of magnitude as that of zeolites [19], which are commonly recognized as materials sensitive to both ionizing and displacement radiation damage. Over the temperature range studied (25–750°C) (especially above room temperature), saponite showed the highest susceptibility to the ionizing irradiation. Although both are dioctahedral smectites, nontronite is more stable than montmorillonite.

As shown both in Table 1 and Fig. 4, all three types of smectites behaved similarly with the increase of temperature. At temperatures in the region between 25°C and 400°C, the amorphization doses of the smectites increased with the increase of temperature. Further increase of temperature leads to a decrease in the amorphization doses. The change of the amorphization dose with temperature of the smectites is different from most other ceramic materials. Wang et al. [21] have reported that, in general, the amorphization dose increases with temperature because of the competition between damage accumulation and annealing of radiation-induced defects. In zeolite phases, however, the critical amorphization dose decreases with the increase of temperature due to the thermal instability of the zeolite framework structures [19].

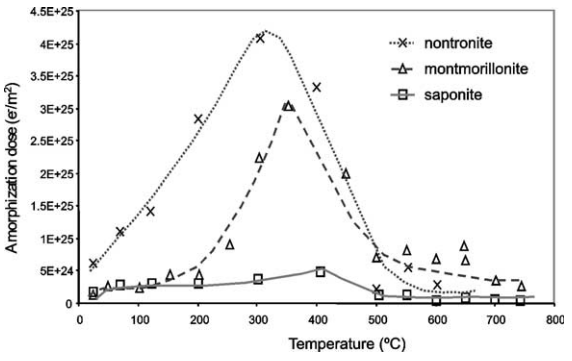

Fig. 4. Temperature dependence of amorphization dose of montmorillonite, nontronite and saponite irradiated by a 200 keV electron beam.

The unique temperature dependence of amorphization dose observed in smectites may be associated with the structural change as a result of heating. Based on the powder X-ray diffraction studies of thermally treated smectites (Figs. 5–7), complete dehydration occurs between 315°C and 410°C for montmorillonite, between 180°C and 300°C for nontronite, and between 225°C and 350°C for saponite. These results are in agreement with the earlier published data using differential thermal analysis (DTA), differential scanning calorimetry (DSC), and emanation thermal analysis (ETA) techniques [14,22]. Based on the thermal analysis with naturally occurring montmorillonite, Bray and Redfern [12] reported that, below 350°C, interlayer water loss is the predominant phenomenon during the thermal treatment. After the removal of interlayer water, further mass loss occurs at temperatures between 430°C and 665°C, over which dehydroxylation becomes important. The dehydration and dehydroxylation of nontronite were found to occur at temperatures of 150°C and 450°C, respectively [23]. Complete dehydroxylation of dioctahedral smectites usually gives rise to a quasi-stable amorphous phase [14] as confirmed in the present study by XRD analysis (Figs. 5 and 6). The dehydration of saponite occurs at ~200°C, whereas the dehydroxylation usually occurs at a temperature 100–200°C higher than that for dioctahedral smectites (~550°C) [29]. The dehydroxylated saponite is unstable and tends to form a new phase, e.g. enstatite, immediately following the completion of dehydroxylation [14]. The increase of amorphization dose with temperature appears to be in the temperature range where dehydration occurs in smectites. Once the temperature reaches the dehydroxylation region of the smectites, the amorphization dose starts to drop with the increase of temperature.

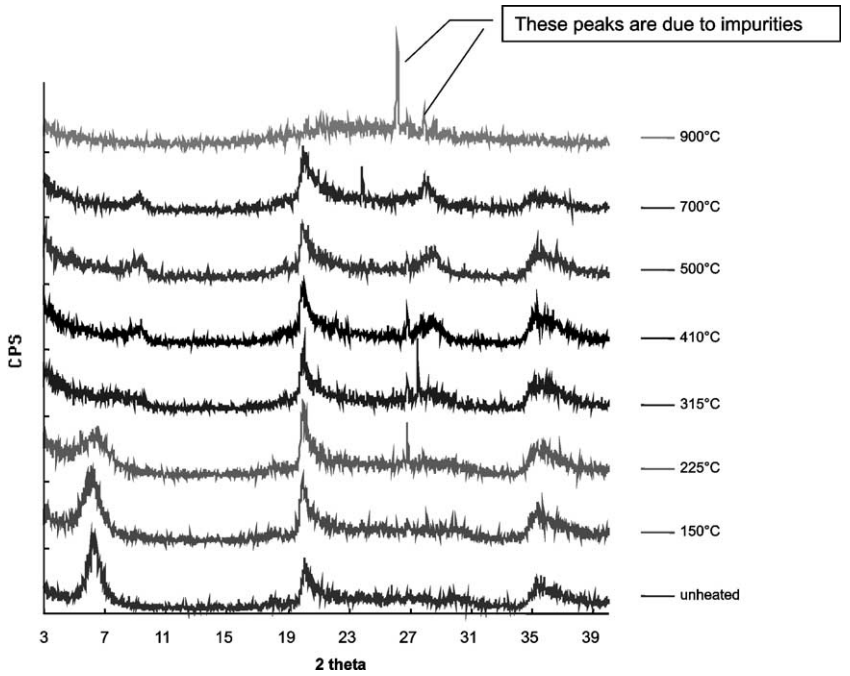

Fig. 5. XRD patterns for montmorillonite heated at temperatures between 150°C and 900°C for 1 h, followed by cooling in air.

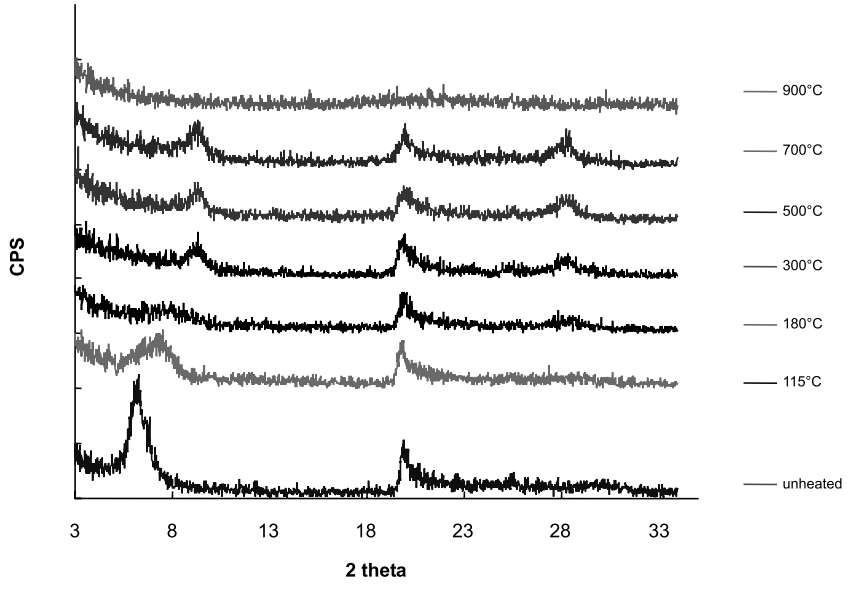

Fig. 6. XRD patterns for nontronite heated at temperatures between 115°C and 900°C for 1 h, followed by cooling in air.

As reported in earlier work [24], the decomposition of structural water by radiolysis induced by incident electrons plays an important role in the disruption of the crystalline structure. The radiation stability of zeolite was found to be significantly increased when the phase was dehydrated [25,26]. The damage mechanisms of zeolite (a hydrated framework structure) by ionization radiation, as proposed by Treacy and Newsam [24] and Wang et al. [19], may be used to explain the damage process of smectites by electron irradiation. The radiolysis of structural water can produce free radicals that attack the bonds in the layered structure. As reported by

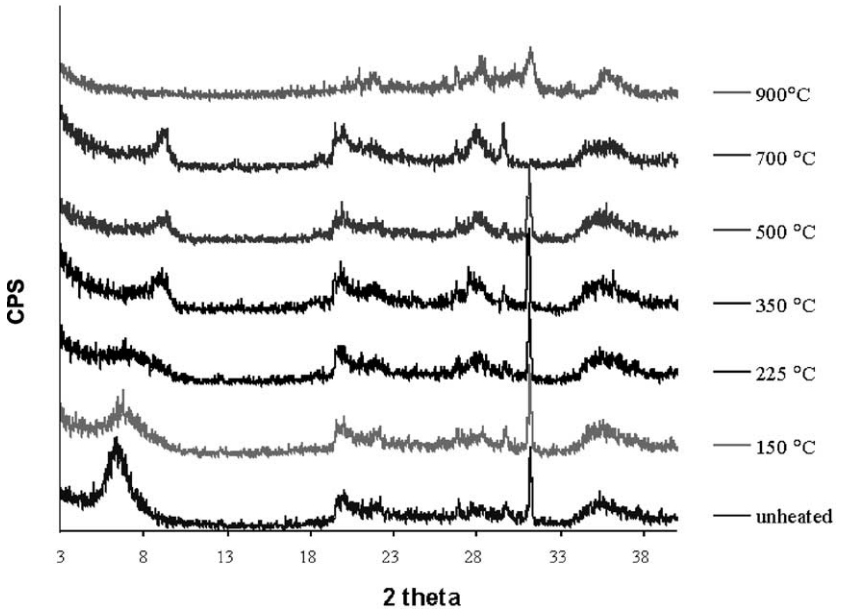

Fig. 7. XRD patterns for saponite heated at temperatures between 150°C and 900°C for 1 h, followed by cooling in air.

Bray and Redfern [12] the amount of water loss in smectite is a function of temperature. With more water being driven off from the interlayer position at higher temperatures, fewer radicals may be produced by radiolysis. Thus, a higher radiation dose is required for the amorphization of the smectite at elevated temperatures.

The displacement of loosely bonded exchangeable cations by electron beam radiation may also contribute to the structural damage. The exchangeable cations may become highly mobile under the impact of the electromagnetic field exerted by the moving electrons and migrate away from the beam interaction region [27]. Because the charge balance in the smectites is delicately maintained by the interlayer cations, the displacement of interlayer cations can cause local charge imbalances that affect the stability of the layered structure. With the removal of interlayer water at elevated temperature, the layer spacing decreases as is evident by the widening and shifting of the first-order diffraction maxima in the X-ray diffraction spectrum to the lower 2θ values (Figs. 5–7). The shorter distance between the negatively charged clay sheet and positively charged interlayer cations leads to a stronger binding force between layers and cations. Furthermore, the dehydration of the smectites is also accompanied by the migration of interlayer cations to the hexagonal cavities in the SiO_4 network. Small interlayer cations may even penetrate the tetrahedral sheet to reside in the octahedral layer sites where they are more tightly bonded to the structure [28]. The difference in bond strength for cations in the interlayer of montmorillonite, nontronite and saponite may explain their different radiation susceptibilities. An earlier study by Malek et al. [29] indicated that the exchangeable cations became fixed at temperatures above 300°C for dioctahedral smectites, such as montmorillonite and beidellite. For trioctahedral smectites, however, the fixation was not complete until the onset of dehydroxylation at temperatures above 700°C [15], because of the strong repulsive electrostatic force of protons of the octahedral sheet hydroxyl ions against the migrated cations. The displacement of interlayer cations is, therefore, easier for saponite (a trioctahedral smectite) than its dioctahedral counterparts, particularly when these materials are dehydrated.

The observed lower amorphization dose in saponite is also attributed to its layer structure. Unlike dioctahedral smectite, whose octahedral layer consists of a large number of vacant sites, saponite has a fully occupied octahedral layer. In dioctahedral smectite, the displaced interlayer cations may move into the vacant sites in the octahedral layer, and the structure remains stable. The migration of interlayer cations into octahedral layer sheet by thermal dehydration is a common phenomenon observed in both dioctahedral and trioctahedral smectites [15,30]. However, the migration of interlayer cations in trioctahedral smectite is usually accompanied by the displacement of structural cations in the octahedral layer, which may make the layered structure unstable [31].

The different radiation stabilities of montmorillonite and nontronite may be attributed to differences in the cation substitutions. The layer charge in nontronite

originates mainly from tetrahedral substitution and may produce a stronger bonding force to the interlayer cation due to a shorter cation-layer distance than for montmorillonite, which has a primarily octahedral substitution. The substitution of Fe for Al in the octahedral layer appears to be another important reason for the enhancement of radiation stability in nontronite. A thermal analysis of nontronite has shown that the Al–O bond was preferentially broken by thermal energy [32] when both Fe and Al were present in the octahedral layer.

The decrease of the amorphization dose in high-temperature regime (400–700°C) is attributed to the thermal instability of the smectites. For dioctahedral smectites, dehydroxylation plays an important role in the thermal stability of the layered structures. When montmorillonite and nontronite are heated to >400°C, the hydroxyl groups in the octahedral sheets interact with one another to form water molecules, and the oxygen ions remain. Based on the model proposed by Drits et al. [33], the structure of the 2:1 layers becomes unstable, and the Al cations tend to migrate to vacant pentagonal prisms formed by oxygen when montmorillonite is dehydroxylated. A study of the dehydroxylation process in the nontronite by Karakassides et al. [32] has shown that the dehydroxylation begins with the loss of OH groups at the Fe–OH–Fe bridges and is completed with the disruption of Al–O bonds. The complete dehydroxylation of dioctahedral smectites was found to result in the formation of quasi-stable amorphous dehydroxylated phases that are rich in defects, such as lattice vacancies [14,29]. A kinetic study of the dehydroxylation process of nontronite [34] showed that the fraction of dehydroxylated phase increased exponentially with increasing temperature, indicating that the thermal stability of dioctahedral smectites degrades with an increase of temperature.

3.2. Ion exchange capacity

The effect of temperature on the ion exchange capacity of smectites was studied with thermally treated smectites at temperatures between 25°C and 900°C. The temperature dependence of the ion exchange capacity for the smectites is shown in Fig. 8. At room temperature, the exchange capacity of the three smectites for Cs is in the order of: montmorillonite (52 mg/g) > nontronite (38 mg/g) > saponite (29 mg/g). In the low-temperature regime (25–400°C), no significant change in the ion exchange capacity was found in any of the three types of smectite. This result indicates that, although the dehydration of smectites can result in the collapse of the interlayer at temperatures between 300°C and 400°C, as indicated by the XRD analysis, the ion exchange capacity can be fully recovered when smectite is saturated in aqueous solution. These results are similar to the

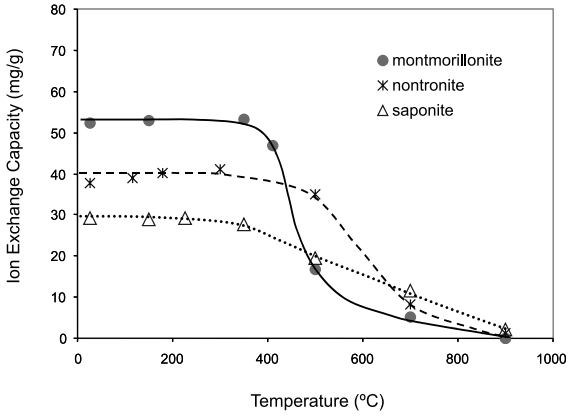

Fig. 8. Temperature dependence of ion exchange capacity of montmorillonite, nontronite and saponite.

observations made by Emmerich et al. [35] for montmorillonites with large interlayer cations, such as Na^+, Ca^{2+} and Sr^{2+}. They reported that montmorillonites with different sizes of interlayer cations showed a different temperature dependence of cation exchange capacity. For montmorillonites with small interlayer cations, such as Cu^{2+} and Li^+, the ion exchange capacity started to decrease at temperatures ~200°C lower than that of the montmorillonite with large interlayer cations, such as Ca^{2+} and Cs^+. This was attributed to the migration and fixation of small cations at the bottom of the hexagonal cavities of the tetrahedral layer or in the octahedral layer sites. The results obtained from the present study suggest that the interlayer cations were not fixed at temperatures below 400°C. The interlayer cations migrated only to the shallow part of hexagonal cavities of the tetrahedral sheet and can be removed from the migrated sites to the exchangeable sites easily when the materials are rehydrated [35]. The ion exchange capacity decreases with increasing temperature when the temperature is above 500°C (Fig. 8). The smectites lose their ion exchange capacity in the high-temperature regime by two processes [30]:

- The exchangeable cations become inaccessible as a result of irreversible collapse of the interlayers. Earlier research has shown that the interlayer of montmorillonite collapsed irreversibly after heating at 350–500°C [36]. This may explain the loss of ion exchange capacity of smectites at temperatures above 400°C.
- The exchangeable cations are fixed at the 'bottom' of the hexagonal cavities of the tetrahedral layer or in the vacant sites of the octahedral layer and become non-exchangeable even if the interlayer space is accessible. This may be the case for saponite. Although saponite swells on rehydration after heating up to 700°C [15], it gradually loses its ion exchange capac-

ity with an increase in temperature at $T > 400$°C. This is because the exchange with the migrated interlayer cations becomes more difficult when the exchangeable cations move 'deeper' into the bottom of hexagonal cavities as temperature increases [37].

Note that once the smectites are amorphized or transformed into a new phase, they lose almost all of their ion exchange capacity. This result suggests that radiation-induced amorphization may also lead to a significant reduction in the ion exchange capacity for radionuclides. This is supported by previous research on radiation- and thermally-amorphized zeolite [16,17], which showed a similar reduction in ion exchange capacity.

4. Conclusions

The structural changes in montmorillonite, nontronite and saponite have been studied using 200 keV electron irradiation. All three types of smectite are susceptible to electron-irradiation-induced amorphization. At room temperature, the amorphization doses of montmorillonite, nontronite and saponite are 1.3×10^{24}, 6.2×10^{24} and 1.7×10^{24} e^-/m^2, which correspond to an energy deposition of 3.0×10^{10}, 3.4×10^{11} and 6.0×10^{10} Gy, respectively. The removal of structural water and the fixation of exchangeable cations appear to be the major reasons for the increase of amorphization dose with increasing temperature in the low-temperature region (25–400°C). At temperatures above 400°C, thermally induced instability of the layered structure due to dehydration and dehydroxylation is responsible for the decrease in amorphization dose.

At room temperature, the ion exchange capacity of the three smectites for Cs is in the order of montmorillonite (52 mg/g) > nontronite (38 mg/g) > saponite (29 mg/g). Thermal treatment does not cause significant loss in the ion exchange capacity at temperatures below 400°C. The amorphization and phase transformations at elevated temperature (900°C) can result in a complete loss of ion exchange capacity.

According to Weber et al. [38], the cumulative dose for commercial high-level waste can reach 10^{10} Gy after 100 years of storage. By comparing the amorphization doses for smectites with the cumulative absorbed dose in the nuclear waste, we may expect the structures of the smectite phases to be partially or completely damaged during storage. This experiment only simulates β-decay effects. During α-decay of trapped radionuclides, local amorphization may occur over even shorter periods of time due to the high mass of decay products, in particular the α-decay recoils (several orders of magnitude heavier than electron). Thus, both radiation and temperature in the near field of a nuclear waste repository may have a significant effect on the structural and chemical properties of smectites.

Acknowledgements

The TEM analysis was conducted at the Electron Microbeam Analysis Laboratory and the neutron activation analysis was performed at the Phoenix Memorial Laboratory at the University of Michigan. The authors thank Dr Shixin Wang for the assistance in performing high-resolution TEM analysis. This work is supported by the Department of Energy's Environmental Management Science Program through grant DE-FG07-97ER45652.

References

[1] D. Savage, The Scientific and Regulatory Basis for the Geological Disposal of Radioactive Waste, Wiley, New York, 1995, p. 83.
[2] F.L. Parker, R.E. Broshears, J. Pasztor, in: The Disposal of High-level Radioactive Waste, A Comparative Analysis of the State-of-Art in Selected Countries, vol. 2, 1984, p. 179.
[3] F. Brandberg, K. Skagius, SKB Technical Report, SKB TR 91-16, 1991.
[4] J.J.W. Higgo, Prog. Nucl. Energy 19 (1987) 173.
[5] A. Lajudie, J. Raynal, J. Petit, P. Toulhoat, Mater. Res. Soc. Symp. Proc. 353 (1995) 221.
[6] M. Takahashi, M. Muroi, A. Inoue, M. Aoki, M. Takizawa, K. Ishigure, N. Fujita, Nucl. Technol. USA 76 (2) (1987) 24.
[7] S.A. Khan, R. Rehman, M.A. Khan, Waste Manage. 15 (8) (1995) 641.
[8] W.L. Gong, L.M. Wang, R.C. Ewing, E. Vernaz, J.K. Bates, W.L. Ebert, J. Nucl. Mater. 254 (1998) 249.
[9] J.A. Fortner, J.K. Bates, Mater. Res. Soc. Symp. Proc. 412 (1996) 205.
[10] T.A. Buscheck, J.J. Nitai, L.D. Rampspott, in: Scientific Basis for Nuclear Waste Management XIX, 1996, p. 715.
[11] R.C. Ewing, W.J. Weber, J.F.W. Clinard, Prog. Nucl. Energy 2 (1995) 63.
[12] H.J. Bray, S.A.T. Redfern, Phys. Chem. Miner. 26 (1999) 591.
[13] R.E. Grim, G. Kulbicki, Am. Mineral. 46 (1961) 1329.
[14] A.C.D. Newman, in: Chemistry of Clays and Clay Minerals, Wiley, New York, 1987, p. 319.
[15] M. Kawano, K. Tomita, Clays Clay Miner. 39 (2) (1991) 174.
[16] B.X. Gu, L.M. Wang, R.C. Ewing, J. Nucl. Mater. 278 (2000) 64.
[17] B.X. Gu, L.M. Wang, S.X. Wang, D.G. Zhao, V.H. Rotberg, R.C. Ewing, J. Mater. Chem. 10 (2000) 2610.
[18] L.M. Wang, S.X. Wang, W.L. Gong, R.C. Ewing, Nucl. Instrum. and Meth. B 141 (1998) 508.
[19] S.X. Wang, L.M. Wang, R.C. Ewing, J. Nucl. Mater. 278 (2000) 233.

[20] W.A. Deer, R.A. Howie, J. Zussman, An Introduction to the Rock-Forming Minerals, 2nd Ed., Longman, London, 1992, p. 369.
[21] L.M. Wang, S.X. Wang, W.L. Gong, R.C. Ewing, W.J. Weber, Mater. Sci. Eng. A 253 (1998) 106.
[22] V.S. Fajnor, K. Jesenak, J. Therm. Anal. 46 (1996) 489.
[23] V. Luca, Clays Clay Miner. 39 (1991) 478.
[24] M.M.J. Treacy, J.M. Newsam, Ultramicroscopy 23 (1987) 411.
[25] R. Csencsits, R. Gronsky, Ultramicroscopy 23 (1987) 421.
[26] L.A. Bursill, E.A. Lodge, J.M. Thomas, Nature 286 (1980) 111.
[27] B.A. Pluijm, J.H. Lee, D.R. Peacor, Clays Clay Miner. 36 (1988) 498.
[28] L. Heller-Kallai, I. Rozenson, Clays Clay Miner. 28 (1980) 355.
[29] Z. Malek, V. Balek, D. Garfinkel-Shweky, S. Yariv, J. Therm. Anal. 48 (1997) 83.
[30] R. Calvet, R. Prost, Clays Clay Miner. 19 (1971) 175.
[31] C. Mosser, L.J. Michot, F. Villeras, M. Romeo, Clays Clay Miner. 45 (1997) 789.
[32] M.A. Karakassides, D. Gournis, T. Simopoulos, D. Petridis, Clays Clay Miner. 48 (2000) 68.
[33] V.A. Drits, G. Besson, F. Muller, Clays Clay Miner. 43 (1995) 718.
[34] N.S. Felix, B.S. Girgis, J. Therm. Anal. 35 (1989) 743.
[35] K. Emmerich, F.T. Madsen, G. Kahr, Clays Clay Miner. 47 (1999) 591.
[36] J. Mering, Trans. Faraday Soc. 42B (1946) 205.
[37] M. Kawano, K. Tomita, Clay Sci. 7 (1989) 277.
[38] W.J. Weber, R.C. Ewing, C.A. Angell, G.W. Arnold, A.N. Cormack, J.M. Delaye, D.L. Griscom, L.W. Hobbs, A. Navrotsky, D.L. Price, A.M. Stoneham, M.C. Weinberg, J. Mater. Res. 12 (1997) 1946.